Ordering and segregation in XPt (X=V, Cu, and Au) random alloys

B. Sanyal* and S. K. Bose†
Physics Department, Brock University, St. Catharines, Ontario, Canada L2S 3A1

V. Drchal and J. Kudrnovský
Institute of Physics, Academy of Sciences of the Czech Republic, 182 21 Prague, Czech Republic
(Received 2 May 2000; revised manuscript received 4 May 2001; published 13 September 2001)

We examine the phase stability and the ordering tendencies of some Pt-based fcc random alloys using the generalized perturbation method (GPM) implemented in the linear muffin-tin orbitals (LMTO) basis. The reference medium for the GPM is chosen as the completely disordered state of the alloy and its electronic structure is described in the coherent potential approximation (CPA). Ordering tendencies and phase stability are examined via effective pair interactions and their lattice Fourier transforms. Relativistic effects on the ground state cohesive properties and the ordering tendencies are determined by carrying out nonrelativistic and fully relativistic (in some cases also scalar-relativistic) LMTO-CPA calculations. In all cases considered, namely XPt with $X=$V, Cu, and Au, the correct ordering tendency is obtained. The ordering tendency is found to be somewhat overestimated in the GPM. Relativistic effects are found to be most prominent in AuPt, where the nonrelativistic LMTO-CPA-GPM description shows a tendency towards $L1_1$ ordering and the correct result, i.e., phase segregation, is obtained only in the fully relativistic description. The sensitivity of the ordering tendency to factors such as lattice relaxation and volume per atom is examined briefly. Finally, the effect on the phase stability of adding a third component, such as V or Au to CuPt alloy, is studied by extending the formalism to the case of a ternary alloy.

DOI: 10.1103/PhysRevB.64.134111 PACS number(s): 71.20.Lp, 64.60.Cn, 71.15.Nc, 71.15.Rf

I. INTRODUCTION

Phase stability of alloys is an important problem from the viewpoint of both theory and practical applications. Numerous methods, with varying degrees of sophistication, have been used to study this problem. Recent studies have involved statistical mechanical models based on reliable calculations of the electronic structure of the alloy.[1,2] Most electronic structure calculations for alloys are either nonrelativistic or scalar relativistic. In this work we consider three platinum-based fcc alloys, VPt, CuPt, and AuPt, and carry out nonrelativistic, scalar-relativistic, and fully relativistic calculations of their electronic structure and the ordering tendency. The method we have chosen to study the ordering tendency is the generalized perturbation method (GPM).[1,3] The reference medium for the GPM is chosen to be the completely disordered state of the alloy. We describe the electronic structure of this (high temperature) disordered state using the coherent potential approximation (CPA) and the linear muffin-tin orbitals (LMTO) basis.[4] The aim of the present work is twofold: (i) to examine the effectiveness of the LMTO-CPA-GPM (Refs. 5–7) method to describe the ordering tendency of a group of Pt-based alloys, showing remarkably different ordering tendencies, and (ii) to study the importance of relativistic effects on the ordering tendency. In addition, we examine the effect of adding Au or V, in small concentrations, on the phase stability of the CuPt alloys.

Several authors have studied ordering behavior of equiatomic Pt-based fcc alloys. Alloys of early $3d$ transition metal (TM) series like $Ti_{50}Pt_{50}$ and $V_{50}Pt_{50}$ show $L1_0$ ordering. Wolverton *et al.* [8] used a cluster expansion technique to determine effective cluster interactions based on direct configurational averaging and the tight-binding linearized muffin-tin orbital (TB-LMTO) method.[4] The results show strong $L1_0$ ordering tendencies, as observed experimentally. Ordering in these alloys can be understood in terms of band-filling arguments,[9,10] which suggest that transition metal (TM) alloys should order if the Fermi energy E_F falls near half filling of their d-band and phase separate if E_F lies near either band edge. Experimentally, alloys within a given TM series are found to obey this trend, although to a lesser extent as we go from $3d$ to the $5d$ series. For isoelectronic TM alloys there are several exceptions to this rule.[9] A notable example is the Ni-Pt alloy, which shows $L1_0$ ordering in equiatomic composition. This system has been studied by several groups[11–17] and in most cases the correct ordering tendency has been obtained, albeit using different methods.

While Ni orders in $L1_0$ structure with Pt, its immediate neighbor Cu orders in $L1_1$ structure. Clark *et al.*[18] calculated the Warren-Cowley short-range order parameter for Cu-Pt, which indicated an instability to concentration fluctuations with a wave vector of $(\frac{1}{2},\frac{1}{2},\frac{1}{2})$, consistent with $L1_1$ ordering. They argued that this ordering vector originates from the large joint density of states associated with L point and X point van Hove singularities which lie near the Fermi energy. While Cu-Au and Cu-Pt both form ordered alloys, Au-Pt shows phase segregation.[17,19] Nonrelativistic calculations for this alloy show a tendency towards ordering, in contradiction to the observed behavior. According to Lu *et al*,[17] charge transfer from the higher Au s-p band into the Pt d band stabilizes the ordered structure in the nonrelativistic description. Relativistic corrections shift the Au s band to deeper binding energies, reducing hybridization between Au s and Pt d bands. There is thus less charge transfer between Au and

 ©2001 The American Physical Society

Pt. They concluded that when both the elements are heavy, relativity promotes phase separation through increased volume deformation energy and diminished charge transfer energy.

In the light of the varied ordering tendencies, ranging from ordering in two different structures ($L1_0$ and $L1_1$) to phase segregation, it is of interest to test the effectiveness of LMTO-CPA-GPM for these Pt-based alloys and to examine the importance of relativistic effects in the phase stability and ordering. In the GPM the difference in the grand potentials (at absolute zero temperature) for the ordered and the completely disordered (random) alloy is cast into an effective Ising model. The parameters of this Ising model, the effective pair interactions (EPI), are a function of band filling and also depend on various other factors, such as volume per atom, and local lattice distortions (relaxations) due to size-mismatch of the constituent atoms. Whenever appropriate and relevant, we examine the effects of these factors on the EPI's and their lattice Fourier transforms. Several drawbacks of this approach should be kept in mind while analyzing the extent of the success or failure of the method. First of all, the use of the single site CPA in describing the disordered state of the alloy completely ignores any chemical short-range order present in the real disordered alloy, which has a significant effect on the relative stability of the ordered and disordered states. Secondly, GPM in its present version does not include the lattice vibration energy. Thus the calculated ordering tendency refers to the instability of the disordered state of the alloy against zero-temperature ordered structure. In addition, any lattice strain energy is also neglected. Finally, the total energy in the grand potential is approximated by the band energy alone. The errors due to the double counting of certain energy terms entering the calculations are assumed to be small by appealing to the so-called ''local force theorem'' of Andersen.[20–22]

II. METHODOLOGY

A. LMTO-CPA-GPM

Nonrelativistic (or scalar-relativistic) (Refs. 5–7) versions of the GPM based on the LMTO-CPA approach have been described in recent publications. A fully relativistic version of LMTO-CPA method is also available.[23] The central idea is the expansion of the thermodynamic potential of the random alloy in a given configuration about a reference medium. The latter is chosen as the completely disordered state of the alloy with its scattering property being described by the coherent potential. The temperature of the system is chosen as the absolute zero, i.e., the entropy effects are neglected. The expansion in occupation indices generates terms dependent on ''pair,'' ''triplet,'' and higher-order ''multiplets'' of atoms. Truncated at the ''pair'' term, the grand potential is identified as a generalized Ising Hamiltonian:

$$H^I = \epsilon_0 + \sum_R \sum_Q D_R^Q \eta_R^Q + \frac{1}{2} \sum_{R,R'} \sum_{Q,Q'} V_{RR'}^{QQ'} \eta_R^Q \eta_{R'}^{Q'} + \cdots, \tag{1}$$

where Q's are the atom species A and B, ϵ_0 is the configuration-independent part of the alloy internal energy, and D_R^Q and $V_{RR'}^{QQ'}$ are the on-site and pair-interaction terms, respectively. η_R^Q's are the occupation indices denoting the probability that the site R is occupied with an atom of type Q. The pair term is important in the present case and it can be evaluated as

$$V_{RR'}^{QQ'} = -\frac{1}{\pi} \lim_{\delta \to 0^+} \int_{-\infty}^{E_F} \mathrm{Im} \times \mathrm{Tr}[t_R^Q(z) \langle g_{R,R'}(z) \rangle t_{R'}^{Q'} \langle g_{R'R}(z) \rangle] dE, \tag{2}$$

where $z = E + i\delta$, and E_F is the Fermi energy. t is the single-site scattering matrix, determined by the potential function $P_R^Q(z)$ for atom type Q at site R, the coherent potential function $\mathcal{P}_R(z)$ and the averaged auxiliary Green function $\langle g(z) \rangle$. The averaged auxiliary Green function $\langle g(z) \rangle$ is completely determined by the coherent potential function and the structure of the underlying lattice.

B. Phase stability in binary and ternary alloys

Binary alloy. Using the lattice gas transformation, the Ising Hamiltonian can be rewritten in terms of the effective pair interactions (EPI) $V_{RR'}$ ($V_{RR'} = V_{RR'}^{AA} + V_{RR'}^{BB} - V_{RR'}^{AB} - V_{RR'}^{BA}$). The ordering tendency of the alloy can be studied by considering the relative strengths of the EPI's for various shells of neighbors, and also by considering their Bloch transform $V(\mathbf{k})$. The occurrence of a deep minimum (with a negative value) in $V(\mathbf{k})$ at a symmetry point of the Brillouin zone of the disordered lattice indicates the instability of the disordered alloy against the ordered structure characterized by the corresponding wave vector.[24] A minimum in $V(\mathbf{k})$ at zero wave vector indicates phase separation. The mean-field spinodal temperature T_0 can be evaluated[24] as

$$T_0 = -\frac{c(1-c)}{k_B} \min V(\mathbf{k}), \tag{3}$$

where c is the concentration and k_B is the Boltzmann constant.

Ternary alloy. A mean-field approach to the phase stability of a ternary alloy was described briefly in one of our earlier publications[25] (in the context of the disordered local moment model of the binary Fe-Al alloy). For the benefit of the readers some details of the method are presented below. Interested readers may also consult the concentration wave approach for multicomponent alloys discussed by Althoff *et al.*[26] and Johnson *et al.*[27] The free energy of the alloy, assuming a pair-summable form for the total energy, can be written as

$$F = \frac{1}{2} \sum_{RR'} \sum_{QQ'} V_{RR'}^{QQ'} \eta_R^Q \eta_{R'}^{Q'} + \Theta \sum_{R,Q} \eta_R^Q \ln(\eta^{Q_R}), \tag{4}$$

where $V_{RR'}^{QQ'}$ is the interaction energy of atoms of types Q and Q' located at sites R and R', respectively. η_R^Q's are occupation indices as described before. Θ is the same as $k_B T$, where

T is the alloy temperature. In the completely disordered state of the alloy $\eta_R^Q = c^Q$, the concentration of atom type Q, independent of the site index R. A general state of the alloy can be viewed as a deviation from this completely disordered state, with $\eta_R^Q = c^Q + \delta\eta_R^Q$. Retaining terms to second order in $\delta\eta_R^Q$,

$$F = F_0 + \frac{1}{2}\sum_{R,R'}\sum_{Q,Q'}\left[V_{RR'}^{QQ'} + \frac{\Theta}{c^Q}\delta_{RR'}\delta_{QQ'}\right]\delta\eta_R^Q\delta\eta_{R'}^{Q'}. \tag{5}$$

Terms linear in $\delta\eta_R^Q$ vanish because of the following constraints: (a) $\Sigma_R \delta\eta_R^Q = 0$ for all Q and (b) $\Sigma_{R'Q'} V_{RR'}^{QQ'} c_{Q'} = \text{const}$ for all R and Q. Taking the Bloch transform of $V_{RR'}^{QQ'}$ and $\delta\eta_R^Q$,

$$F = F_0 + \frac{1}{2}\sum_{\mathbf{k}}\sum_{Q,Q'}\left[V^{QQ'}(\mathbf{k}) + \frac{\Theta}{c^Q}\delta_{QQ'}\right] \times [\delta\eta^Q(\mathbf{k})]^* \delta\eta^{Q'}(\mathbf{k}), \tag{6}$$

with $\Sigma_Q \delta\eta^Q(\mathbf{k}) = 0$ for all $\mathbf{k}$. The free energy of the alloy with respect to the completely disordered state, $\Delta F = F - F_0$, is a quadratic form in $\delta\eta^Q(\mathbf{k})$. For high Θ it is positive definite. With decreasing temperature Θ, it can cease to be positive definite. This condition leads to the required eigenvalue problem for the critical temperature.

We define a concentration matrix in terms of the concentrations of A, B, and C types of atoms as

$$c = \begin{pmatrix} c_A & 0 & 0 \\ 0 & c_B & 0 \\ 0 & 0 & c_C \end{pmatrix}.$$

Concentration fluctuations can be expressed in a matrix form as

$$\begin{pmatrix} \delta\eta^A \\ \delta\eta^B \\ \delta\eta^C \end{pmatrix} = \delta\eta(\mathbf{k})Y(\mathbf{k}) = \delta\eta(\mathbf{k})\begin{pmatrix} y^A(\mathbf{k}) \\ y^B(\mathbf{k}) \\ y^C(\mathbf{k}) \end{pmatrix},$$

while the pair interactions form a 3×3 matrix

$$V = \begin{pmatrix} V^{AA}(\mathbf{k}) & V^{AB}(\mathbf{k}) & V^{AC}(\mathbf{k}) \\ V^{BA}(\mathbf{k}) & V^{BB}(\mathbf{k}) & V^{BC}(\mathbf{k}) \\ V^{CA}(\mathbf{k}) & V^{CB}(\mathbf{k}) & V^{CC}(\mathbf{k}) \end{pmatrix}.$$

In terms of these matrices

$$\Delta F = \frac{1}{2}\sum_{\mathbf{k}}^{(\mathrm{BZ})} Y^\dagger(\mathbf{k})[V(\mathbf{k}) + \Theta c^{-1}]Y(\mathbf{k})|\delta\eta(\mathbf{k})|^2. \tag{7}$$

BZ denotes the first Brillouin zone of the disordered lattice. One has to find the largest value of Θ for which $\lambda(\mathbf{k}) = 0$ for some $\mathbf{k}$ by solving the eigenvalue problem

$$[V(\mathbf{k}) + \Theta c^{-1}]Y(\mathbf{k}) = \lambda(\mathbf{k})Y(\mathbf{k}), \quad \sum_Q y^Q(\mathbf{k}) = 0. \tag{8}$$

These can be rewritten as

$$\tilde{V}X = -\Theta X, \quad \sum_Q \sqrt{c_Q x_Q} = 0, \tag{9}$$

where $\tilde{V} = c^{1/2} V c^{1/2}$ and $X = c^{-1/2} Y$.

The above 3×3 eigenvalue problem along with the subsidiary condition $\Sigma_Q \sqrt{c_Q x_Q} = 0$, can be converted into a 2×2 eigenvalue problem without any subsidiary condition by introducing an orthonormal basis of vectors

$$e_0 = \begin{pmatrix} \sqrt{c_A} \\ \sqrt{c_B} \\ \sqrt{c_C} \end{pmatrix}, \quad e_1 = \begin{pmatrix} \sqrt{\dfrac{c_B}{c_A + c_B}} \\ -\sqrt{\dfrac{c_A}{c_A + c_B}} \\ 0 \end{pmatrix},$$

$$e_2 = \begin{pmatrix} \sqrt{\dfrac{c_A c_C}{c_A + c_B}} \\ \sqrt{\dfrac{c_B c_C}{c_A + c_B}} \\ -\sqrt{c_A + c_B} \end{pmatrix},$$

with $e_i^T e_j = \delta_{ij}(i,j = 0,1,2)$ and $e_0^T X = 0$ where T is the transpose. In this basis,

$$\tilde{\mathcal{V}}\begin{pmatrix} \zeta \\ \xi \end{pmatrix} = -\Theta\begin{pmatrix} \zeta \\ \xi \end{pmatrix}, \tag{10}$$

where $\tilde{\mathcal{V}} = e_i^T \tilde{V} e_j (i,j = 1,2), X = \xi e_1 + \zeta e_2$. The largest eigenvalue Θ of the above equation yields the spinodal temperature T_0. The wave vector $\mathbf{k}_0$ corresponding to this largest eigenvalue determines the nature of the transition. If $\mathbf{k}_0$ is a symmetry point of the BZ of the disordered lattice, then the disordered state is unstable against the ordered state generated by the concentration wave of wave vector $\mathbf{k}_0$. If $\mathbf{k}_0 = 0$, then the disordered state is unstable against the segregated phase.

III. RESULTS AND DISCUSSION

A. Binary alloys

We have determined the equilibrium lattice parameters of the random alloys using the fully relativistic and nonrelativistic LMTO-CPA methods in the atomic sphere approximation (ASA).[4] Phase stabilities of these alloys were studied at these equilibrium (minimum energy) lattice constants. The exchange correlation functional used in most of our calculations is that due to Ceperley and Alder[28] as parametrized by Perdew and Zunger.[29] In all calculations the maximum angular momentum quantum number l was restricted to 2 and core orbitals were determined self-consistently (all-electron calculations). $\mathbf{k}$ space integrations were performed over the

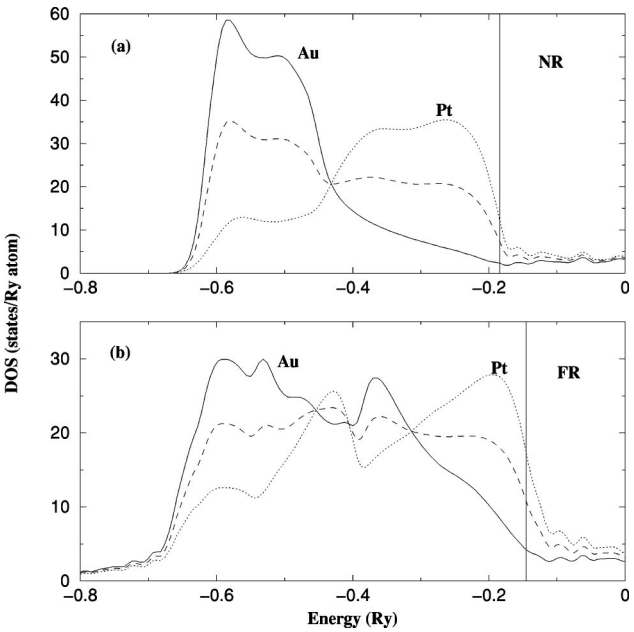

FIG. 1. Partial and averaged densities of states of AuPt alloy for the (a) nonrelativistic and (b) fully relativistic cases (bold lines: Au PDOS; dotted lines: Pt PDOS; dashed lines: averaged DOS). Vertical lines show the positions of the Fermi levels.

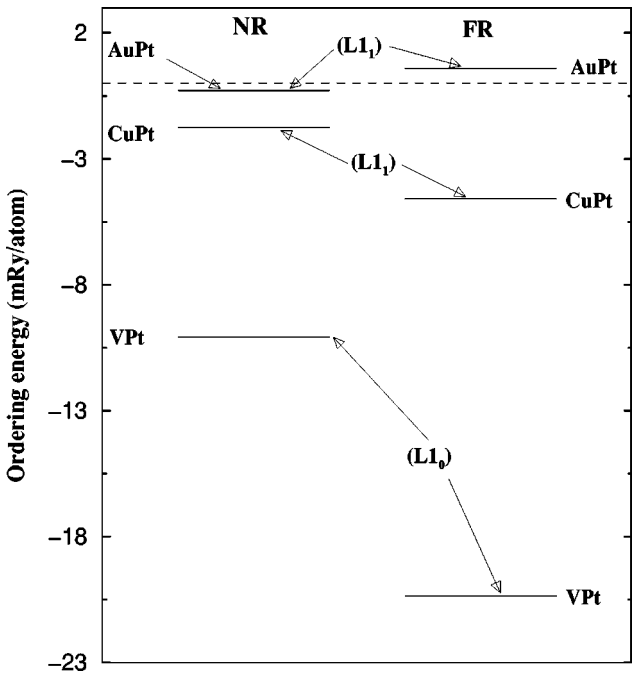

FIG. 2. Schematic diagram showing the ordering energies of the alloys in the nonrelativistic (NR) and fully relativistic (FR) treatments. The ordered structures for which the ordering energies are calculated [using Eqs. (11) or (12)] are shown.

irreducible wedge of the Brillouin zone using 280 **k** points. Energy integrations were performed using a semicircle contour in the complex energy plane for 12 points. In all the calculations, we included the lattice relaxation effects using the approximate treatment suggested by Kudrnovský and Drchal.[30] Also, to avoid having to compute the Madelung energy, the constituent spheres were made charge neutral (with charge transfer $\sim 1/10\,000$th of an electron). The choices of radii were made carefully to insure that the sphere overlaps stay within the range of validity of ASA.

For the binary alloys scalar-relativistic calculations were performed in addition to nonrelativistic and fully relativistic calculations. Scalar-relativistic results were found to be intermediate between the nonrelativistic and fully relativistic results, as expected. In all cases, relativistic effects reduce the equilibrium lattice constants and increase the bulk moduli, e.g., from 1.66 MBar (nonrelativistic) to 2.45 MBar (fully relativistic) in case of $Au_{50}Pt_{50}$. As expected, the smallest difference between the lattice parameters in the nonrelativistic and fully relativistic treatments is obtained for VPt (2.67%). The largest difference is for AuPt, 5.25%. For CuPt the difference is about 3%. The actual values of the nonrelativistic (NR) and fully relativistic (FR) lattice parameters in atomic units are 7.459,7.265 (VPt); 7.391,7.165 (CuPt); and 8.127,7.721 (AuPt), respectively. In all cases Vegard's[31] or Zen's[32,33] law values for the lattice parameters are found to be closer to the FR values than the NR values. The Vegard's and Zen's law lattice parameters for a given alloy are found to be almost identical.

In $Au_{50}Pt_{50}$ relativistic effects cause (i) significant downward shift in the energies of *s* and *p* states, as revealed by the changes in the *s*- and *p*-partial DOS's projected on Au and Pt atoms, and (ii) a broadening of the *d*-band, with both Au and Pt projected *d* partial DOS's showing this trend (Fig. 1). Total bandwidth increases as a result. In spite of the broadening of the bands there is an increase in the DOS at the Fermi level, increasing the band energy. This results in an upward shift of the ordering energy (positive in this case), which is reflected in turn in an increase in the segregation tendency of the alloy. Spin-orbit coupling introduces additional structure (peaks) in the DOS. PDOS for Au has $d_{3/2}$ and $d_{5/2}$ states around -0.55 Ryd and -0.35 Ryd, respectively, which can be seen in Fig. 1(b). For Pt, this happens for -0.45 Ryd and -0.2 Ryd. Similar spin-orbit coupling induced structures are observed in the two other alloys studied, the change with respect to the nonrelativistic case being of course the most pronounced in case of $Au_{50}Pt_{50}$. However, the effect of mass velocity and Darwin terms as well as the spin-orbit coupling on the band and ordering energies is quite the opposite. In VPt and CuPt (where the alloy shows ordering) the relativistic effects cause a downward shift in the ordering energy, increasing the ordering tendency.

The ordering energies E_{ord} based on EPI's up to the fourth neighbor shell[34]

$$E_{\mathrm{ord}} = -\tfrac{1}{2}V_1 + \tfrac{3}{4}V_2 - V_3 + \tfrac{3}{2}V_4 \quad (L1_0) \tag{11}$$

$$= -\tfrac{3}{4}V_2 + \tfrac{3}{2}V_4 \quad (L1_1) \tag{12}$$

are shown in Fig. 2, where the corresponding structures for which the ordering energies were calculated are also shown. A positive (negative) ordering energy indicates segregation (ordering). The behavior of Au-Pt is in sharp contrast with the other two alloys. The EPI's for the first and second near-

TABLE I. Effective pair interactions (EPI) for first and second nearest neighbor shells (V_1 and V_2) in nonrelativistic (NR) and fully relativistic (FR) treatments.

Alloy system	EPI (in mRyd/atom)			
	NR		FR	
	V_1	V_2	V_1	V_2
VPt	9.566	−3.378	25.686	−4.749
CuPt	8.753	2.214	6.498	3.308
AuPt	1.135	1.865	−2.276	1.154

est neighbor shells, obtained in nonrelativistic and fully relativistic treatments, are given in Table I. Except for AuPt, the nearest neighbor EPI is much larger than the next nearest neighbor EPI. For VPt the nearest neighbor EPI V_1 increases in the relativistic description. Thus for VPt, which shows $L1_0$ ordering dominated by first neighbor EPI V_1 [Eq. (11)], the ordering energy becomes more negative in the relativistic treatment. CuPt shows $L1_1$ ordering and here the ordering energy is dictated by second neighbor EPI V_2 [Eq. (12)]. Relativistic effects increase V_2 (Table I) for this alloy and thus increase the $L1_1$ ordering tendency. For AuPt the ordering energy is negative in the nonrelativistic treatment and becomes positive in the fully relativistic treatment. The inclusion of scalar relativistic effects, i.e., the mass velocity and Darwin terms, changes the sign of the nearest neighbor EPI in AuPt [see Fig. 3(a)] from positive to negative. However, the ordering energy still remains negative. Only in the fully relativistic treatment does the ordering energy become positive. For AuPt the nearest and next nearest neighbor EPI's (V_1 and V_2) are of comparable magnitude. Although the nearest neighbor EPI changes its sign from positive to negative upon inclusion of the scalar-relativistic effects, contributing towards a tendency to phase segregation [see Fig. 3(a)], the second neighbor EPI V_2 still remains sufficiently positive to yield the $L1_1$ long-range order. The segregation tendency further increases in the fully relativistic treatment (with the inclusion of spin-orbit interaction) due to further lowering of both V_1 and V_2. For the $L1_0$ structure a positive value for the EPI at the second neighbor shell encourages segregation by promoting *A*-*B* pairs at the second shell, effectively increasing the probability of *A*-*A* or *B*-*B* pairs at the nearest neighbor sites. Thus VPt the positive value of V_1 and the negative value of V_2 both promote ordering in the $L1_0$ structure.

In Fig. 3 we provide a comparison of the EPI's and ETI's for AuPt for the nonrelativistic (NR), scalar relativistic (SR), and fully relativistic (FR) treatments. The object is twofold: to show the relative magnitudes of the EPI's and the ETI's, and to show the change from NR to SR and from SR to FR treatment. The EPI's corresponding to further neighbors and the effective triplet interactions (ETI) may play a significant role for weakly ordered or segregated alloys, in general when the band-filling is such that the Fermi level is close to a minimum of the nearest neighbor EPI, V_1. Thus of the alloys studied in this work ETI's may be of some importance only in AuPt. The upper panel (a) of Fig. 3 shows the EPI's in AuPt and also the corresponding ordering vector $\mathbf{k}_0$ at which

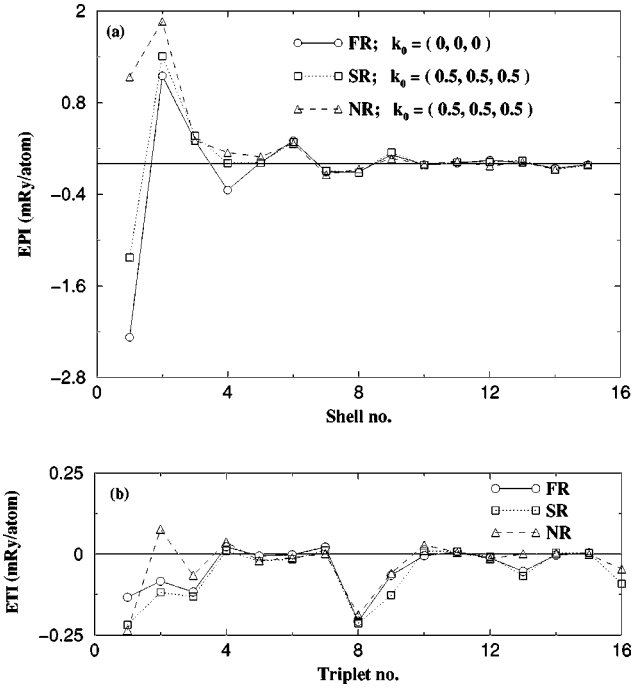

FIG. 3. Effective (a) pair and (b) triplet interactions in AuPt obtained via nonrelativistic (NR), scalar-relativistic (SR) and fully relativistic (FR) LMTO-CPA-GPM. Pair interactions are shown as a function of the various neighbor shells at which they are calculated. See text (Sec. III A) for the description of some of the triplets for which the ETI's are shown in panel (b). The ordering vectors $\mathbf{k}_0$ [panel (a)] for the three cases are in units of $2\pi/a$, where a is the lattice parameter of the underlying fcc lattice.

the lattice Fourier transform of the EPI's $V(\mathbf{k})$ has its minimum. $V(\mathbf{k})$ was calculated by considering the EPI's up to the 15th neighbor shell. Figure 3 shows that the differences among the NR, SR, and FR treatments are appreciable only up to the fourth shell EPI, V_4. Also, beyond the 6th shell the EPI's are negligible and have little effect on the ordering tendency. For the nonrelativistic (NR) treatment $V(\mathbf{k})$ has its minimum at the symmetry point L of the Brillouin zone of the fcc lattice [(0.5, 0.5, 0.5) in units of $2\pi/a$, where a is the fcc lattice parameter], indicating that the $L1_1$ ordered structure is stable against the disordered state. The scalar-relativistic treatment changes the sign of the nearest neighbor EPI from positive to negative, suppressing the formation of the nearest neighbor *A*-*B* pair. However, the second neighbor EPI remains sufficiently positive to yield a negative ordering energy for the $L1_1$ structure. Thus even in the SR treatment the ordering vector stays at (0.5, 0.5, 0.5). Only in the fully relativistic treatment does the ordering vector $\mathbf{k}_0$ reduce to (0, 0, 0), showing the stability of the segregated phase against the disordered alloy. More accurate full potential total energy calculations by Lu *et al.*[17] show that scalar-relativistic corrections (mass velocity and Darwin) already yield the correct ground state (phase separation) for the AuPt alloy at equiatomic composition. As pointed out in the last paragraph of Sec. I (Introduction) one source of error in the GPM lies in approximating the total energy difference by the difference in the band energy alone. The use of the atomic

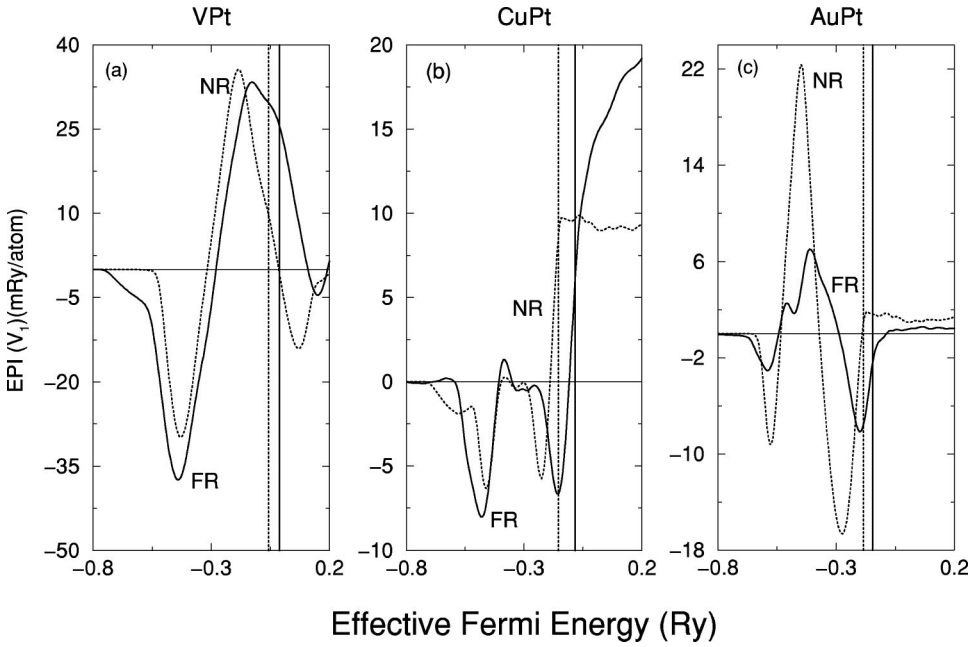

FIG. 4. Nearest neighbor effective pair interactions (V_1) vs effective Fermi energies for the nonrelativistic (NR) and fully relativistic (FR) cases: (a) VPt, (b) CuPt, and (c) AuPt. The bold and the dotted lines show the positions of Fermi energies for the fully relativistic and nonrelativistic cases, respectively.

sphere approximation (ASA), which replaces the full potential with a spherical approximation in our implementation of the LMTO method, leads to additional errors. Our scalar-relativistic result for AuPt showing a tendency to ordering is similar to that obtained by Watson *et al.*[35] using the linearized Slater-type-orbital (LASTO) method. Their scalar-relativistic calculation, based on spherical potentials, yields a negative enthalpy of formation for AuPt in the B_2 structure.

The lower panel (b) of Fig. 3 shows the ETI's for various triplets. Only a few ETI's are comparable in magnitude to the EPI's up to the 6th neighbor shell. The triplet no. 1 is composed entirely of nearest neighbors, i.e., the three pairs involved are the nearest neighbors of each other. The second triplet consists of two nearest neighbor pairs and one second neighbor pair. The third triplet consists of two nearest neighbor pairs and one third neighbor pair. Triplet no. 8, the triplet with the largest magnitude, consists of the linear array of atoms along the face diagonal of the conventional cubic cell. Triplet no. 9 is the triangle formed by two edges and the face diagonal of the conventional cube. The fact that the shortest linear triplet is of the largest magnitude is due to the angular dependence of the hopping or transfer integrals. This result is consistent with the general trend in the relative strength of various multiatom interactions discussed by Bieber and Gautier.[36] Further discussion on the relativistic effects in AuPt and its qualitative difference with respect to other alloys studied in this work is provided at a later point.

Of the three alloys studied the strongest ordering tendency is obtained for $V_{50}Pt_{50}$. This is of course also the alloy where the usual band-filling argument would suggest a strong ordering tendency. Fully relativistic treatment increases the ordering tendency, with the ordering energy becoming more negative compared with its nonrelativistic value. This can be seen from Fig. 4(a) where the energy-dependent first neighbor effective pair interaction (V_1) is plotted. In Fig. 5 energy-dependent effective pair interactions, up to the fourth nearest neighbor shell, are shown as a function of varying Fermi energy E [i.e., calculated by replacing the upper limit in the integral in Eq. (6) by E]. It is seen that all other EPI's become irrelevant compared to the first nearest-neighbor EPI in this strongly ordered alloy. Ordering in VPt is mainly governed by the nearest neighbor pair interaction V_1, which is 3–5 times larger than the second neighbor EPI (Table I), and several orders of magnitude larger than the more distant ones. The wave vector corresponding to the minimum of $V(\mathbf{k})$ is (1,0,0), indicating $L1_0$ type ordering. This is in accordance with the results obtained by Wolverton *et al.*[8] using the cluster expansion method in the TB-LMTO basis. Calculated spinodal temperature T_0 varies from $\sim$3200 K (NR) to $\sim$6500 K (FR), grossly

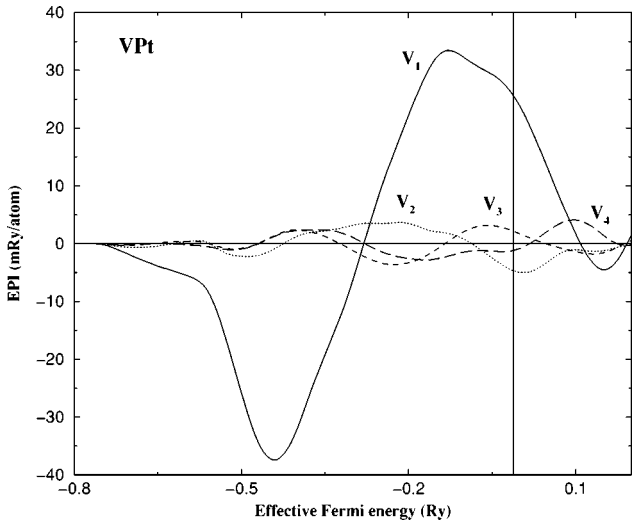

FIG. 5. Effective pair interactions (EPI) for VPt in fully relativistic treatment. Bold, dotted, dashed, and long-dashed lines correspond to V_1, V_2, V_3, and V_4, respectively, where V_n is the EPI for the nth neighbor shell. The vertical line shows the position of the Fermi level.

overestimated values, partly due to the mean-field approximation [Eq. (3)] but mainly due to the fact that EPI's are overestimated in GPM, some reasons for which have been discussed in one of our earlier publications.[25] In this case, diagonal disorder (large difference in the centers of the *d*-bands of the two components) drives the system towards ordering.

For comparison with VPt, in Figs. 4(b) and 4(c) we present the energy-dependent first neighbor EPI's for CuPt and AuPt, respectively. Figure 4 clearly shows the nontrivial differences in the shape of the energy-dependent first neighbor EPI's of the three alloys. There is no generic shape, which could be used together with band-filling arguments, to understand the ordering in all three alloys. This is not surprising, as such arguments usually apply to alloys across a given transition metal (TM) series only. In addition, the validity of such arguments is often limited to a few adjacent members of a given TM series. Note that for the $L1_1$ ordering of CuPt the decrease in V_1 due to relativistic effects shown in Fig. 4(b) is irrelevant. As mentioned earlier, the increased ordering tendency in the FR treatment for CuPt results from an increase in the second neighbor EPI V_2, as shown in Table I. The ordering energy in this case is governed by V_2 and V_4 [see Eq. (12)]. Since V_4 is much smaller than V_2, the change in the latter dictates the change in its ordering tendency.

$Cu_{50}Pt_{50}$ is unique in the sense that it is the only Pt-based fcc metallic alloy that shows $L1_1$ ordering with alternating fcc (1, 1, 1) layers of Cu and Pt.[18] Clark *et al.*[18] have shown that the stability of CuPt in $L1_1$ ordered structure is due to van Hove–like singularities at two high-symmetry points *X* and *L*. The spanning vector between *X* and *L* is $(\frac{1}{2},\frac{1}{2},\frac{1}{2})$, which is a member of the star of *L*, the ordering vector for $L1_1$ structure. The results obtained by Clark *et al.*[18] (as well as by Pinski *et al.*[12] for NiPt) are not based on the decomposition of electronic energy into pairwise contributions. They, in effect, contain all higher order interactions. Our calculations, based on pair interactions only, lead to very similar results. The wave vector corresponding to the minimum of $V(\mathbf{k})$ is found to be $(\frac{1}{2},\frac{1}{2},\frac{1}{2})$, showing $L1_1$ ordering in both nonrelativistic and fully relativistic treatments. The spinodal temperature T_0 varies from ~1200 K (NR) to ~1600 K (FR).

For alloys between transition metals and Pt relativistic effects increase the value of V_1, while for alloys between noble metals and Pt relativistic effects reduce the value of V_1. This effect becomes more prominent as one goes down the noble metal column to Ag and Au and one finds that relativity leads to increasingly clustering tendencies. The effect is prominent in AuPt. Pt and the transition metals have *d*-like states at the Fermi level. The noble metals have *s*-like states at the Fermi level. Relativistic effects shift the noble metal *s*-band to deeper binding energies, making it less able to provide charge to the Pt *d*-band. The potential parameter *C* in the LMTO Hamiltonian, which is a measure of the center of the band, is −0.39 Ry and −0.58 Ry for nonrelativistic and fully relativistic Au *s*-bands, respectively. Thus, as noted earlier by Lu *et al.*,[17] decreased charge transfer from noble metal *s*- (and *p*-) band to the Pt *d*-band makes the ordered structure less stable in a relativistic description. The effect is the opposite for alloys of Pt with transition metals where the states at the Fermi level are *d*-like.

TABLE II. Effective pair interactions (EPI) for first to fourth nearest neighbor shells (V_1 to V_4) and lattice Fourier transform of EPI's [$V(\mathbf{k})$], calculated by considering EPI's up to the fifteenth neighbor shell, for AuPt alloy in fully relativistic (FR) treatment, for three different lattice parameters. "Eq." denotes the equilibrium lattice parameter.

	Lattice parameters (in a.u.)		
	7.22	7.72 (eq.)	8.20
V_1	−3.273	−2.276	−1.753
V_2	1.049	1.154	1.046
V_3	0.517	0.302	0.185
V_4	−0.654	−0.346	−0.172
$V(\mathbf{k})$	−0.033	−0.020	−0.014

All results presented so far were calculated by considering the lattice relaxation effects in the disordered state in an approximate way as suggested by Kudrnovský and Drchal.[30] In general, the inclusion of lattice relaxation decreases the disordered state (CPA) energy. Thus with lattice relaxation, the system has a diminished tendency to move away from the disordered state into an ordered state. According to Eqs. (1) and (2) this means that EPI's calculated in the unrelaxed state are higher.

Volume per atom has a noticeable effect on the calculated EPI's (see Table II). In general, as the volume per atom increases, the nearest neighbor EPI acquires a positive shift. For AuPt this results in a diminished segregation tendency, while for all other alloys studied this means an increased ordering tendency. Increased volume per atom results in less hybridization and less charge transfer, both of which increases the disordered state energy, resulting in a positive shift of the EPI.

B. Ternary alloys

In this section, we present some results on the changes in phase stability of a binary alloy such as CuPt with the gradual addition of a third component. The results presented are for scalar-relativistic calculations and charge neutral spheres, with lattice relaxation taken into account as in previous cases. In all calculations, the ternary alloy has been modeled to be $A_{(1-x)/2}B_{(1-x)/2}C_x$ where *C* is the component which is added to the *A*-*B* alloy in equiatomic composition. Vegard's law has been assumed for the lattice constants of these ternary alloys. We have chosen V and Au to be the third component to be added gradually to the CuPt alloy. This choice was motivated by the fact that simple band-filling arguments[9,10] would dictate that the addition of V (Au) should lead to an increase (decrease) in the ordering tendency. However, changes in the ordering tendency are somewhat complicated by the fact that while VPt orders, Cu and V are immiscible. Similarly, while Au-Pt segregates, Cu-Au orders—making it worthwhile studying the changes in the

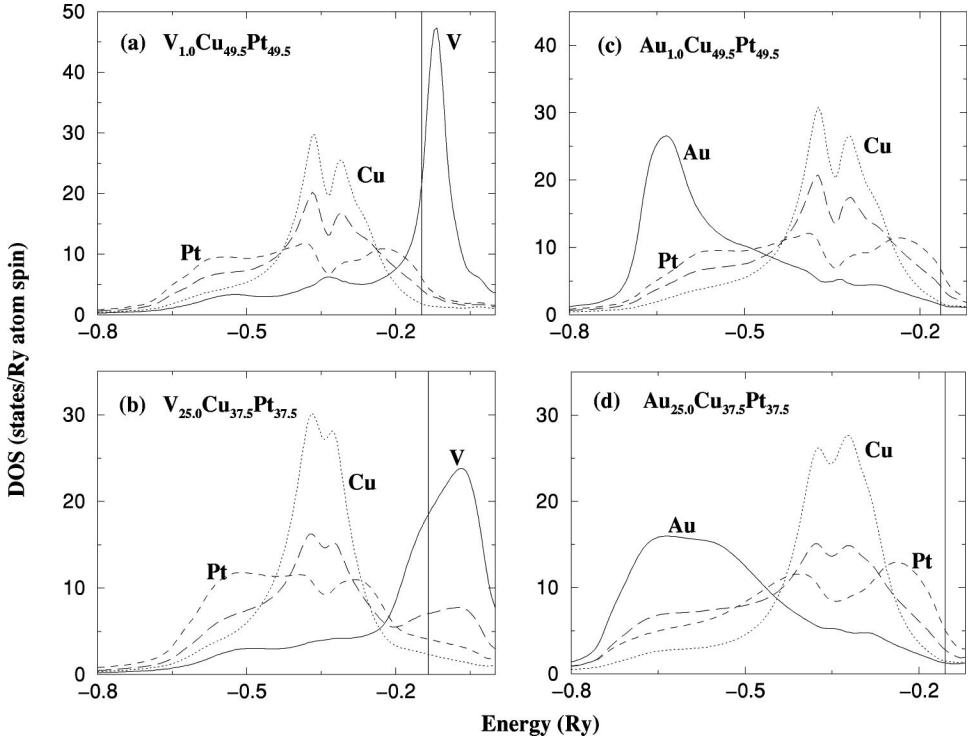

FIG. 6. Partial and averaged DOS's for the ternary alloys: (a) $V_{1.0}Cu_{49.5}Pt_{49.5}$, (b) $V_{25}Cu_{37.5}Pt_{37.5}$, (c) $Au_{1.0}Cu_{49.5}Pt_{49.5}$, and (d) $Au_{25}Cu_{37.5}Pt_{37.5}$. [Bold: V(Au) partial DOS; dotted: Cu DOS; dashed: Pt DOS, long-dashed: averaged DOS]. Vertical lines show the position of Fermi levels.

ordering tendency in CuPt as a result of the addition of Au. Partial and averaged DOS's for some of the ternary alloys are presented in Figs. 6(a)–6(d). In Fig. 6(a), the DOS's of the ternary alloy $V_{1.0}Cu_{49.5}Pt_{49.5}$ are shown. The effect of adding V is to create an impurity-type peak above the Fermi level, widely separated from the bulk of the Cu and Pt DOS's. With increasing concentration of V this peak becomes broader and hybridizes with Cu and Pt bands [see Fig. 6(b), where V is 25%). Figure 7 shows the effect of V addition on the nearest neighbor Cu-Pt EPI. We have seen that in pure $Cu_{50}Pt_{50}$ alloy $(\frac{1}{2},\frac{1}{2},\frac{1}{2})$ ordering exists and the nearest neighbor EPI's are positive. When V is gradually added to CuPt the value of nearest neighbor Cu-Pt EPI increases at first up to $\sim$ 5% V and then decreases. This is also reflected in the ordering wave vector which changes from $(\frac{1}{2},\frac{1}{2},\frac{1}{2})$ to (0,0,0), indicating a transition from ordering to segregation. This transition is possible for a very small concentration of V, since V and Cu are immiscible. Calculation for a binary $Cu_{1-x}V_x$ alloy, with $x\sim5\%$, indeed shows a very large segregation temperature ($\sim$16 000 K). In the ternary CuPtV alloy (with small V concentration) the nearest neighbor EPI between Cu and V has a high negative value (approximately -11 mRyd). This supersedes the positive EPI between Cu and Pt.

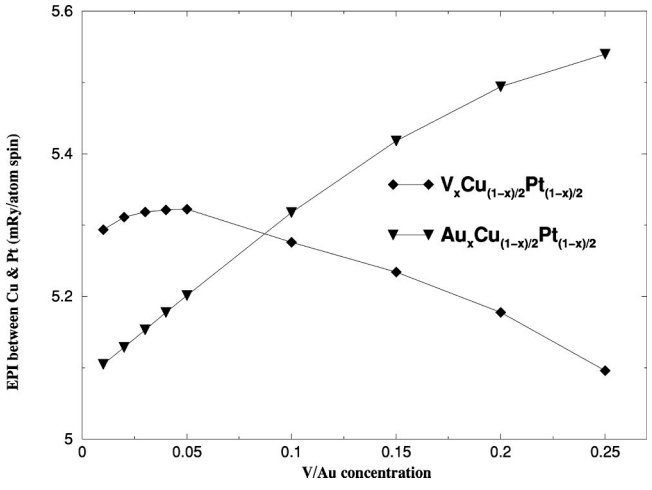

FIG. 7. Effective pair interactions (EPI) between Cu and Pt atoms in ternary alloys vs concentration of the third component. The curve joining the diamonds is for V in CuPt alloy, while the curve joining the triangles is for Au in CuPt.

In (c) and (d) of Fig. 6, the alloys shown are $Au_{1.0}Cu_{49.5}Pt_{49.5}$ and $Au_{25}Cu_{37.5}Pt_{37.5}$, respectively. For low concentration of Au (1%), the impurity peak is well below the peaks of Cu and Pt and wider due to the *s*-character of Au. As the concentration of Au increases there is increasing hybridization of Au bands with those of Pt and Cu. We see a gradual increase in ordering tendency as the EPI between Cu and Pt increases with the increasing concentration of Au. The ordering vector changes from $(\frac{1}{2},\frac{1}{2},\frac{1}{2})$ to (1,0,0) around 10% of Au. This is understandable, as the $(\frac{1}{2},\frac{1}{2},\frac{1}{2})$ ordering of CuPt is not particularly stable, being dependent on van Hove–like singularities at *X* and *L* points of the Brillouin zone of the disordered lattice. As discussed by Clark *et al.*,[18] with a change in the Fermi level, or equivalently electron per

atom ratio (e/a), this ordering can change either to clustering or (1,0,0) type ordering. Our GPM calculation yields a spinodal temperature of 1830 K for 25% Au while for binary $Cu_{50}Pt_{50}$, it yields a value of 1600 K.

As an application of the ternary alloy formulation presented in Sec. II B we have also examined the effect of putting 1% vacancy in CuPt alloy. Results for EPI's show that the ordering tendency is increased in the presence of vacancies. The first nearest neighbor EPI (V_1) between Cu and Pt increases by 3% in the presence of vacancies. There is a corresponding increase of 12% in ordering temperature. The ordering vector still stays at $(\frac{1}{2},\frac{1}{2},\frac{1}{2})$. The 12% increase in the ordering temperature accompanying a 3% increase in the nearest neighbor EPI simply reflects the fact that the EPI's involving further neighbors cannot be ignored for this ternary case. All lattice Fourier transforms for the ternary alloy calculation were obtained by including the EPI's up to the fifteenth neighbor shell. The relationship between the ordering temperature and the EPI for the case of ternary alloy is not exactly linear, as shown in Sec. II B. The results for the 1% vacancy in CuPt indicates that vacancies may play an important role in ordering. Although experimental investigations of the role of vacancies in ordering in some alloys have been carried out,[37] theoretical studies in this regard are lacking. We are currently carrying out a detailed study of the role of vacancies in ordering in binary alloys.

IV. CONCLUSION

We have presented results related to the phase stability of three Pt-based alloys using nonrelativistic and fully relativistic TB-LMTO-CPA-GPM method. Two of these alloys, VPt and CuPt, are known to order in $L1_0$ and $L1_1$ structures, respectively, while AuPt phase segregates. Our calculated results for these alloys, showing remarkably different ordering tendencies, are in agreement with existing experimental observation. We have shown that relativistic effects are important for these Pt-based alloys, particularly for AuPt. Our calculations for ternary alloys show some interesting trends, which are amenable to experimental verification. The existing body of experimental data is insufficient in this regard.

ACKNOWLEDGMENTS

Financial support for this work was provided by the Natural Sciences and Engineering Research Council of Canada.

*Current address: Condensed Matter Theory Group, Department of Physics, Uppsala University, Box 530, 75121 Uppsala, Sweden. Email address: biplab@fysik.uu.se

†Email address: bose@newton.physics.brocku.ca

[1] F. Ducastelle, in *Order and Phase Stability in Alloys*, edited by F. de. Boer and D. Pettifor (North-Holland, Amsterdam, 1991).

[2] *Alloy Phase Stability*, edited by G. Stocks and A. Gonis (Kluwer Academic, Dordrecht, 1989).

[3] F. Ducastelle and F. Gautier, J. Phys. F: Met. Phys. **6**, 2039 (1976); see also F. Gautier, in *High Temperature Alloys: Theory and Design*, edited by J. O. Stiegler (The Metallurgical Society of AIME, Philadelphia, PA, 1984), p. 163.

[4] (a) O. K. Andersen, O. Jepsen, and M. Sob, in *Electronic Structure and its Applications*, edited by M. Youssouff, Lecture Notes in Physics Vol. 283 (Springer, Berlin, 1987), pp. 1–57; (b) O. K. Andersen, O. Jepsen, and D. Glotzel, in *Highlights of Condensed Matter Theory*, edited by F. Bassani, F. Fumi, and M. P. Tosi (North-Holland, Amsterdam, 1985), pp. 59–176.

[5] V. Drchal, J. Kudrnovský, L. Udvardi, P. Weinberger, and A. Pasturel, Phys. Rev. B **45**, 14 328 (1992).

[6] J. Kudrnovský, S.K. Bose, and V. Drchal, Phys. Rev. Lett. **69**, 308 (1992).

[7] A. Pasturel, V. Drchal, J. Kudrnovský, and P. Weinberger, Phys. Rev. B **48**, 2704 (1993).

[8] C. Wolverton, G. Ceder, D. de Fontaine, and H. Dreysse, Phys. Rev. B **48**, 726 (1993).

[9] A. Bieber and F. Gautier, Acta Metall. **34**, 2291 (1986).

[10] V. Heine and J. Samson, J. Phys. F: Met. Phys. **13**, 2155 (1983).

[11] C. Amador and G. Bozzolo, Phys. Rev. B **49**, 956 (1994).

[12] F. J. Pinski, B. Ginatempo, D. D. Johnson, J. B. Staunton, G. M. Stocks, and B. L. Gyorffy, Phys. Rev. Lett. **66**, 766 (1991).

[13] Z. W. Lu, S.-H. Wei, and A. Zunger, Phys. Rev. Lett. **66**, 1753 (1991).

[14] C. Amador, W. R. L. Lambrecht, M. van Schilfgaarde, and B. Segall, Phys. Rev. B **47**, 15 276 (1993).

[15] A. V. Ruban, I. A. Abrikosov, and H. L. Skriver, Phys. Rev. B **51**, 12 958 (1995).

[16] P. P. Singh, A. Gonis, and P. E. A. Turchi, Phys. Rev. Lett. **71**, 1605 (1993).

[17] Z. W. Lu, S.-H. Wei, and A. Zunger, Europhys. Lett. **21**, 221 (1993).

[18] J. F. Clark, F.J. Pinski, P. A. Sterne, D. D. Johnson, J. B. Staunton, and B. Ginatempo, in *Metallic Alloys: Experimental and Theoretical Perspectives*, edited by J. S. Faulkner and R. G. Gordan (Kluwer Academic, Netherlands, 1994), p. 159; J. F. Clark, F.J. Pinski, D. D. Johnson, P. A. Sterne, J. B. Staunton, and B. Ginatempo, Phys. Rev. Lett. **74**, 3225 (1995).

[19] I. A. Abrikosov and H. L. Skriver, Phys. Rev. B **47**, 16 532 (1993).

[20] A.R. Mackintosh and O.K. Andersen, *Electrons at the Fermi Surface*, edited by M. Springford (Cambridge University Press, Cambridge, England, 1980), p. 149.

[21] V. Heine, in *Solid State Physics: Advances in Research and Applications*, edited by H. Ehrenreich, F. Seitz, and D. Turnbull (Academic, New York, 1980), p. 1.

[22] M. Methfessel, and J. Kübler, J. Phys. F: Met. Phys. **12**, 141 (1982).

[23] V. Drchal, J. Kudrnovský, and P. Weinberger, Phys. Rev. B **50**, 7903 (1994).

[24] A. G. Khachaturyan, *Theory of Structural Transformations in Solids* (Wiley, New York, 1983).

[25] S.K. Bose, V. Drchal, J. Kudrnovský, O. Jepsen, and O.K. Andersen, Phys. Rev. B **55**, 8184 (1997); S.K. Bose, J. Kudrnovský, V. Drchal, O. Jepsen, and O.K. Andersen, Mater. Sci. Eng., B **37**, 237 (1996).

[26] J.D. Althoff, D.D. Johnson, F.J. Pinski, and J.B. Staunton, Phys. Rev. B **53**, 10 610 (1996).

[27] D.D. Johnson, M. Asta, and J.D. Althoff, Philos. Mag. Lett. **79**, 551 (1999).
[28] D. M. Ceperley and B. J. Alder, Phys. Rev. Lett. **45**, 566 (1980).
[29] J. Perdew and A. Zunger, Phys. Rev. B **23**, 5048 (1981).
[30] J. Kudrnovský and V. Drchal, Phys. Rev. B **41**, 7515 (1990).
[31] L. Vegard, Z. Phys. **5**, 17 (1921).
[32] E-an Zen, Am. Mineral. **41**, 523 (1956).
[33] J. Hafner, *From Hamiltonians to Phase Diagrams*, Springer Series in Solid-State Sciences Vol. 70 (Springer-Verlag, Berlin, 1987), p. 147.
[34] P. Weinberger, V. Drchal, L. Szunyogh, J. Fritscher, and B. I. Bennett, Phys. Rev. B **49**, 13 366 (1994).
[35] R. E. Watson, J. W. Davenport, and M. Weinert, Phys. Rev. B **35**, 508 (1987).
[36] A. Bieber and F. Gautier, J. Phys. Soc. Jpn. **53**, 2061 (1984).
[37] K. Chattopadhyay, S. Lele, N. Thangaraj, and S. Ranganathan, Acta Metall. **35**, 727 (1987).